LETTER

doi:10.1038/nature10194

Excitatory transmission from the amygdala to nucleus accumbens facilitates reward seeking

Garret D. Stuber[1,2], Dennis R. Sparta[1,2], Alice M. Stamatakis[1], Wieke A. van Leeuwen[2], Juanita E. Hardjoprajitno[2], Saemi Cho[2], Kay M. Tye[2,3], Kimberly A. Kempadoo[2], Feng Zhang[3], Karl Deisseroth[3] & Antonello Bonci[2,4]

The basolateral amygdala (BLA) has a crucial role in emotional learning irrespective of valence[1–5,21–23]. The BLA projection to the nucleus accumbens (NAc) is thought to modulate cue-triggered motivated behaviours[4,6,7,24,25], but our understanding of the interaction between these two brain regions has been limited by the inability to manipulate neural-circuit elements of this pathway selectively during behaviour. To circumvent this limitation, we used *in vivo* optogenetic stimulation or inhibition of glutamatergic fibres from the BLA to the NAc, coupled with intracranial pharmacology and *ex vivo* electrophysiology. Here we show that optical stimulation of the pathway from the BLA to the NAc in mice reinforces behavioural responding to earn additional optical stimulation of these synaptic inputs. Optical stimulation of these glutamatergic fibres required intra-NAc dopamine D1-type receptor signalling, but not D2-type receptor signalling. Brief optical inhibition of fibres from the BLA to the NAc reduced cue-evoked intake of sucrose, demonstrating an important role of this specific pathway in controlling naturally occurring reward-related behaviour. Moreover, although optical stimulation of glutamatergic fibres from the medial prefrontal cortex to the NAc also elicited reliable excitatory synaptic responses, optical self-stimulation behaviour was not observed by activation of this pathway. These data indicate that whereas the BLA is important for processing both positive and negative affect, the glutamatergic pathway from the BLA to the NAc, in conjunction with dopamine signalling in the NAc, promotes motivated behavioural responding. Thus, optogenetic manipulation of anatomically distinct synaptic inputs to the NAc reveals functionally distinct properties of these inputs in controlling reward-seeking behaviours.

To stimulate excitatory fibres projecting from the BLA to the NAc selectively, we stereotaxically delivered adeno-associated viral vectors carrying the codon-optimized *channelrhodopsin*-2 gene fused in-frame to enhanced yellow fluorescent protein (*ChR2–EYFP*)[8], driven by the *Camk2α* promoter, to transduce glutamatergic neurons locally in the BLA. Expression of ChR2–EYFP was observed after transduction of neurons in the BLA (Fig. 1a). Whole-cell recordings from visually identified BLA pyramidal neurons expressing ChR2 showed that light stimulation frequencies (1–20 Hz, 5-ms light pulses) resulted in reliable firing in response to light, with minimal loss of spike fidelity at 20 Hz (Fig. 1b and Supplementary Fig. 1). This indicated that optically induced firing via activation of ChR2 can excite BLA neurons at physiologically relevant frequencies[5,6]. Expression of ChR2–EYFP was observed in targets of the BLA in the forebrain, including the NAc (Fig. 1c). Optical stimulation of ChR2–EYFP-positive fibres and synaptic terminals from the BLA to the NAc resulted in excitatory responses in the NAc (Fig. 1d and Supplementary Fig. 2). Light-evoked excitatory postsynaptic currents (EPSCs) from visually identified medium spiny neurons were blocked by bath application of the competitive α-amino-3-hydroxy-5-methyl-4-isoxazolepropionic acid receptor (AMPAR) antagonist 6-cyano-7-nitroquinoxaline-2,3-dione (CNQX) at 10 μM, demonstrating that optical stimulation of BLA-to-NAc fibres results in AMPAR-mediated EPSCs via the release of synaptic glutamate (Fig. 1d).

To test whether selective activation of BLA-to-NAc synapses could promote motivated behavioural responding, mice injected into the BLA with viruses encoding ChR2–EYFP or EYFP alone (control) were stereotactically implanted with a guide cannula above the ipsilateral NAc. At 21–28 d after surgery, a fibre-optic cable connected to a laser capable of activating ChR2 was positioned directly above the NAc for optical stimulation (Supplementary Fig. 3). Mice were then placed in behavioural testing chambers equipped with two ports: an active port, which when triggered by beam-breaks from nose-poke responses, produced an optical stimulation train to activate BLA-to-NAc fibres

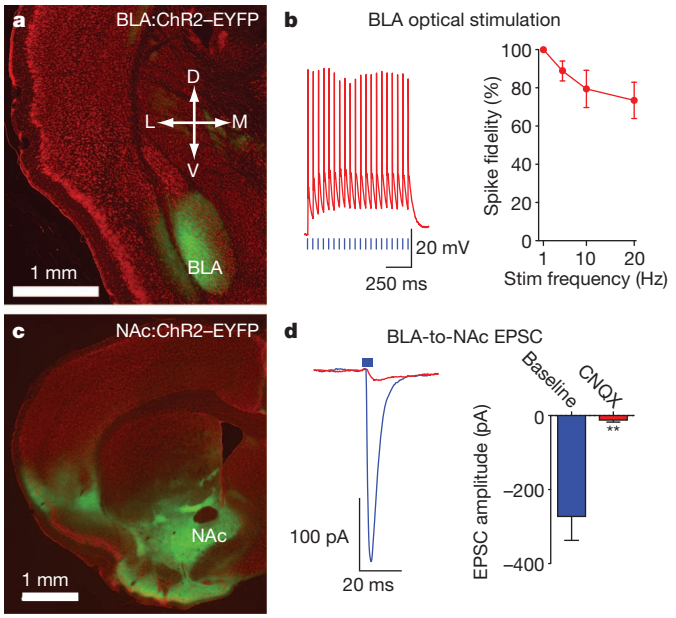

Figure 1 | Expression of ChR2–EYFP in BLA neurons and fibres projecting to the NAc. **a**, Coronal brain slice stained with red fluorescent Nissl stain, showing expression of ChR2–EYFP (green) after virus injection into the BLA. D, dorsal; V, ventral; M, medial; L, lateral. **b**, Example traces and average data for action potentials in current-clamped ChR2-expressing BLA neurons in response to 5-ms light pulses ($n = 7$ cells, $P = 0.015$). **c**, Brain slice showing expression of ChR2–EYFP in the NAc after virus injection into the BLA. **d**, EPSCs recorded from NAc neurons after optical stimulation of BLA-to-NAc fibres before and after bath application of CNQX ($n = 4$ cells, $P = 0.007$). All error bars for all figures correspond to the s.e.m.

[1]Department of Psychiatry and Department of Cell and Molecular Physiology, UNC Neuroscience Center, University of North Carolina at Chapel Hill, Chapel Hill, North Carolina 27599, USA. [2]Ernest Gallo Clinic and Research Center, Department of Neurology, Wheeler Center for the Neurobiology of Drug Addiction, University of California San Francisco, San Francisco, California 94608, USA. [3]Department of Bioengineering and Department of Psychiatry and Behavioral Sciences, Stanford University, Stanford, California 94305, USA. [4]Intramural Research Program, National Institute on Drug Abuse, Baltimore, Maryland 21224, USA.

selectively, and an inactive port which produced no optical stimulation. Mice expressing ChR2–EYFP in BLA-to-NAc terminals readily learned to perform nose-poke responses to earn optical stimulations in a single 60-min behavioural session, in contrast to EYFP-expressing control mice (Fig. 2a, b, Supplementary Fig. 4 and Supplementary Movie 1). Inactive nose-poke responses were not significantly different between mice expressing ChR2–EYFP and EYFP alone, indicating that optical stimulation of BLA-to-NAc fibres did not cause an increase in general responding (Fig. 2b). In contrast, direct optical activation of BLA cell bodies was highly variable in promoting self-stimulation behaviour (Supplementary Fig. 5).

To determine whether optical stimulation of BLA-to-NAc fibres reinforced nose-poke behaviour and thus increased the likelihood of additional behavioural responses, laser stimulations were withheld while active nose-poke responses were recorded in a behavioural session. Mice expressing ChR2–EYFP showed a significant decrease

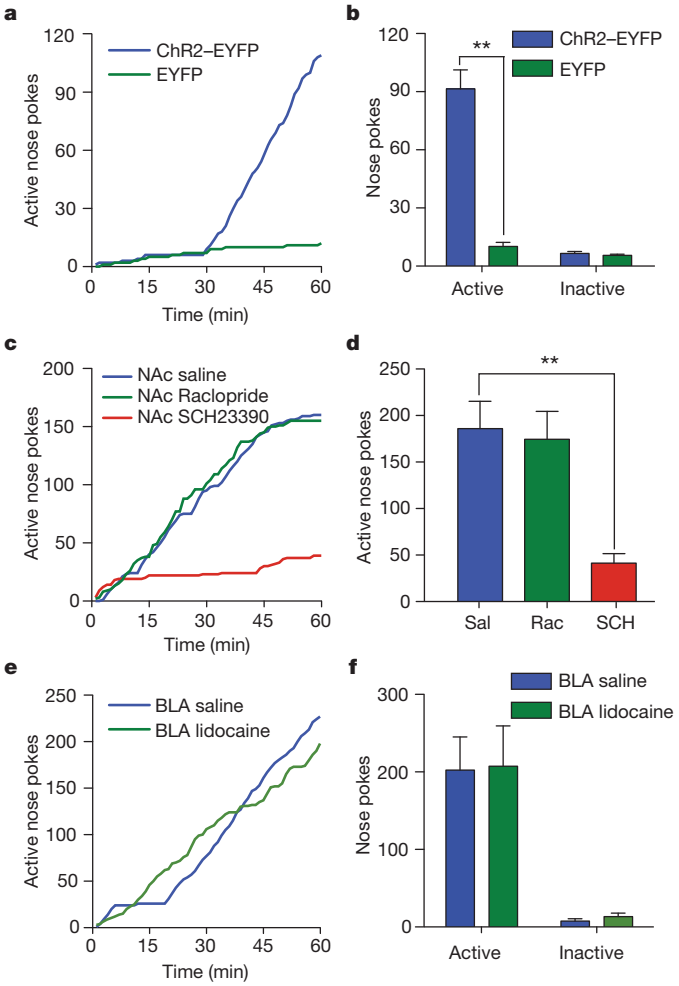

Figure 2 | *In vivo* optical activation of BLA-to-NAc fibres promotes self-stimulation. **a**, Example cumulative-activity graphs of active nose pokes made in the first behavioural session to obtain optical stimulation of BLA-to-NAc fibres in a ChR2–EYFP-expressing mouse and a control (EYFP-expressing) mouse. **b**, Average numbers of nose pokes during the first optical self-stimulation session ($n = 12$ ChR2–EYFP mice; $n = 10$ EYFP mice; **, $P < 0.0001$). **c**, Example cumulative-activity graphs of nose pokes made for optical stimulation after unilateral intra-NAc microinjections of saline, raclopride or SCH23390. **d**, Average numbers of nose pokes after intra-NAc microinjections of saline (Sal), raclopride (Rac) or SCH23390 (SCH) ($n = 19$ saline, $n = 11$ SCH23390, $n = 20$ raclopride; **, $P = 0.0016$). **e**, Example cumulative-activity graphs of active nose pokes made for optical stimulation in mice that received intra-BLA vehicle or lidocaine. **f**, Average numbers of nose pokes after intra-BLA injection of vehicle or lidocaine ($n = 6$ intra-BLA saline group; $n = 6$ intra-BLA lidocaine, $P = 0.88$).

in responding when optical stimulations were withheld for 1 h (Supplementary Fig. 6). In addition, mice showed a rapid renewal of self-stimulation behaviour when optical stimuli were delivered non-contingently, and subsequent nose-poke responses were again reinforced after the 1-h extinction period.

Many forms of motivated behaviour depend on dopaminergic[9–11] as well as glutamatergic signalling in the NAc[6,7,12]. To test whether optical self-stimulation behaviour of BLA-to-NAc fibres was dependent on dopaminergic signalling, mice trained previously in the optical self-stimulation task were given microinjections into the NAc (through the same guide cannula used to introduce the optical fibre) of either vehicle, a dopamine D1-type receptor (D1R) antagonist, SCH23390, or a dopamine D2-type receptor (D2R) antagonist, raclopride, immediately before optical self-stimulation sessions. D2R antagonism (tested at two doses, Supplementary Fig. 7) had no effect, whereas D1R antagonism markedly decreased the number of active nose pokes (Fig. 2c, d). D1R antagonism did not reduce the rate of responding in the beginning of the behavioural session, nor did it affect the rate of responding within a burst of nose pokes, indicating that decreased responding during the entire session was not due to locomotor impairments induced by unilateral D1R antagonism (Supplementary Fig. 8). Notably, application of SCH23390 to NAc brain slices expressing ChR2 in BLA-to-NAc fibres markedly decreased the amplitude of all EPSCs evoked by the same optical stimulation train (60 pulses at 20 Hz) that reinforced nose-poking behaviour (Supplementary Fig. 9). These data indicate that the reinforcing properties of BLA-to-NAc stimulation require glutamate release from BLA fibres, which has postsynaptic effects on medium spiny neurons that are modulated by D1Rs.

Activation of BLA-to-NAc fibres may produce action potentials that propagate back to cell bodies in the BLA and could then activate axon collaterals that project to other brain regions. Therefore, in mice trained previously to self-stimulate, we tested whether BLA-to-NAc optical self-stimulation required neural activity in the BLA, by inactivating it with intracranial injections of lidocaine immediately before self-stimulation sessions. Ipsilateral inactivation of the BLA had no effect on acquisition (Supplementary Fig. 10) or expression of optical self-stimulation behaviour (Fig. 2e, f), demonstrating that the reinforcing properties of the optical stimulation were mediated by BLA glutamatergic fibres in the NAc or by fibre collaterals outside the BLA.

To determine whether the activity of BLA-to-NAc fibres was required for naturally occurring motivational processing, we performed pathway-specific optical inactivation experiments in a separate behavioural task in which mice were trained to drink a sucrose solution in response to a reward-predictive cue. The BLA was bilaterally injected with a virus encoding the light-gated Cl^- pump, *Natronomonas pharaonis* halorhodopsin (NpHR)[13] (AAV-Camk2α–eNpHR3.0–EYFP; Supplementary Fig. 11). Whole-cell recordings from brain slices containing NpHR-expressing BLA neurons showed that 500-ms pulses of 532-nm light delivered to the slice resulted in prominent outward currents (146.2 ± 61.4 pA; $n = 5$ cells) when neurons were voltage-clamped at −60 mV. Current injections that reliably produced trains of action potentials were inefficient at eliciting spiking when NpHR was activated (Fig. 3a). In a subset of mice in which BLA neurons were transduced with viruses to express both ChR2 and NpHR, stimulation of BLA-to-NAc fibres via activation of ChR2 with 473-nm light resulted in light-evoked EPSCs, as predicted. However, when NpHR was simultaneously active in BLA-to-NAc fibres, ChR2 activation resulted in markedly more failed EPSCs (Fig. 3b). Thus, NpHR activation was capable of reducing evoked BLA-to-NAc EPSCs, and should therefore also reduce the endogenous activity of BLA-to-NAc fibres *in vivo*.

Mice with optical fibres implanted above the NAc and expressing NpHR in BLA-to-NAc fibres underwent four conditioning sessions consisting of 50 trials in which a 5-s tone and house-light stimulus predicted the delivery of 20 μl of 20% sucrose. Motivated behavioural

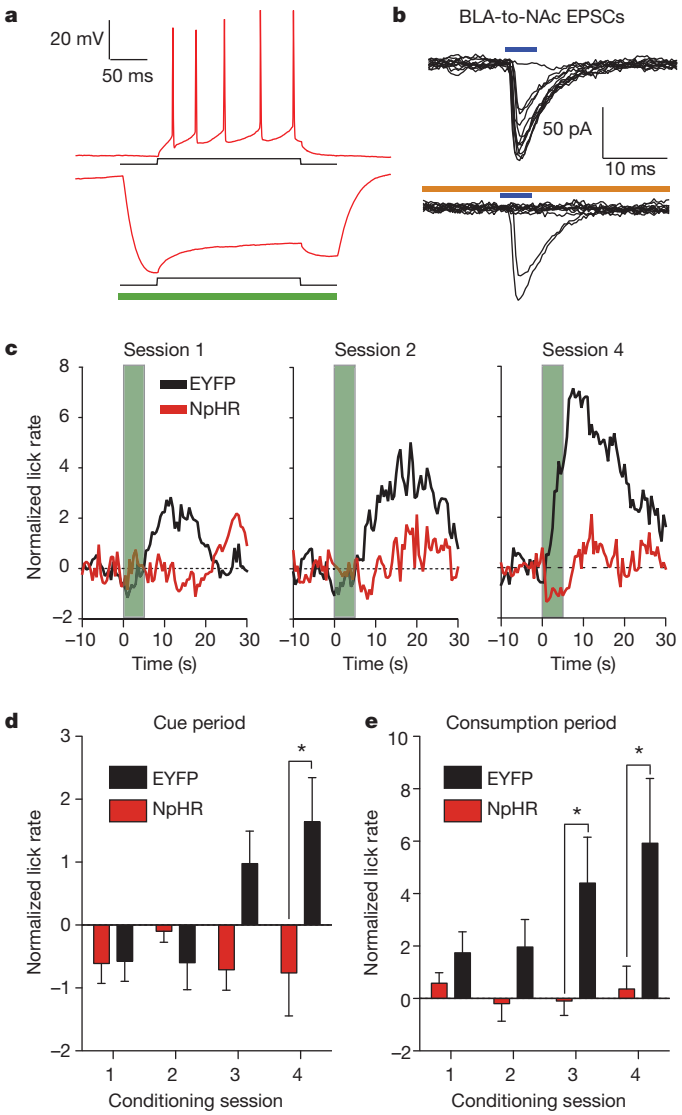

Figure 3 | *In vivo* optical inactivation of BLA-to-NAc fibres reduces behavioural responding for sucrose. **a**, Injection of 100 pA current for 200 ms into NpHR-expressing neurons in the BLA results in reliable spiking of BLA neurons (6.6 ± 0.9 spikes). In all neurons, NpHR-mediated hyperpolarization completely blocked spikes due to the current injection ($P = 0.02$, $n = 3$). **b**, ChR2 (473 nm)-evoked EPSCs at BLA-to-NAc synapses are reduced when NpHR is activated (593.5 nm) in the same pathway. **c**, Average normalized lick rates (*Z*-score), time-locked to cue onset ($t = 0$–5 s, green bar) and sucrose delivery ($t = 5$ s), for NpHR-expressing and EYFP-expressing mice. BLA-to-NAc fibres were transiently inactivated (from $t = -0.2$ s to $t = 5.2$ s) in NpHR-expressing mice on each trial of each conditioning session. **d**, **e**, Data from panel **c** divided into time bins corresponding to the cue period ($t = 0$–5 s) or the sucrose consumption period ($t = 5$–15 s). Lick rates were significantly attenuated during the cue period (**d**) in mice receiving BLA-to-NAc inhibition ($P = 0.013$ for treatment, $n = 7$ mice per group). Lick rates were also significantly reduced during the sucrose consumption period (**e**) ($P = 0.001$ for treatment, $n = 7$ mice per group).

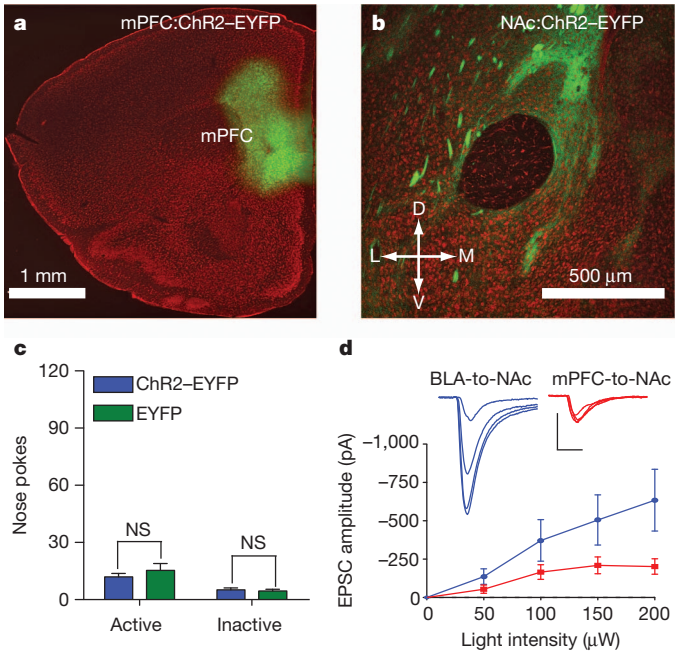

Figure 4 | *In vivo* optical activation of mPFC-to-NAc fibres does not promote self-stimulation. **a**, Coronal brain slice stained with red fluorescent Nissl showing expression of ChR2–EYFP (green) after virus injection into the mPFC. **b**, Expression of ChR2–EYFP in fibres originating in the mPFC and innervating the NAc. **c**, Average numbers of nose pokes made by mice expressing ChR2–EYFP in mPFC-to-NAc fibres and by control (EYFP-expressing) mice ($n = 12$ ChR2–EYFP mice; $n = 10$ EYFP mice; NS, not significant, $P = 0.333$). **d**, EPSCs recorded from NAc neurons, evoked by either mPFC-to-NAc or BLA-to-NAc optical stimulation at increasing light intensities ($n = 7$ cells per group; effect for stimulated input, $P = 0.003$).

responding was assayed by the number of licks that each mouse made at the sucrose receptacle. On each cue–reward pairing, BLA-to-NAc fibres were transiently inactivated by delivering laser pulses bilaterally 200 ms before cue onset and terminating these pulses 200 ms after the end of the cue (laser on for 5.4 s per trial, Supplementary Fig. 12). Laser illumination was delivered in an identical fashion to control mice expressing only EYFP. Over the four conditioning sessions, control mice developed robust time-locked licking behaviour in response to the reward-predictive stimulus as well as to subsequent sucrose delivery (Fig. 3c–e). In contrast, mice that received transient inhibition of BLA-to-NAc fibres during the cue–reward pairing period showed a marked attenuation of licking in response to the cue or to subsequent reward delivery (Fig. 3c–e). Transient BLA-to-NAc inactivation during cue–reward pairing also reduced the total number of licks throughout the entire session. However, when NpHR-expressing mice underwent an additional sucrose-responding session, but without laser inhibition of the BLA-to-NAc fibres, the amount of licking in the session returned to levels similar to those observed in control mice, demonstrating that the presence of NpHR alone (without optical modulation) was not sufficient to alter licking behaviour (Supplementary Fig. 13). These data show that brief, transient inhibition of BLA-to-NAc fibres can reduce motivated behavioural responding to obtain natural rewards.

In addition to the glutamatergic projection from the BLA, the NAc receives excitatory synaptic inputs from infralimbic and prelimbic regions of the medial prefrontal cortex (mPFC)[14] that are thought to modulate compulsive reward-seeking behaviour[15,16]. To determine whether activation of mPFC-to-NAc excitatory synaptic connections promotes reward-seeking behaviour similarly to BLA-to-NAc activation, mice were injected into the mPFC with ChR2–EYFP virus (Fig. 4a). This resulted in expression of ChR2–EYFP in fibres in the NAc (Fig. 4b). Mice were then tested to determine whether optical activation of mPFC-to-NAc fibres (Supplementary Fig. 14) supported self-stimulation behaviour similar to that caused by BLA-to-NAc activation. Notably, mice expressing ChR2–EYFP at mPFC-to-NAc connections showed no difference in the numbers of active or inactive nose pokes made relative to EYFP-expressing control mice (Fig. 4c). ChR2–EYFP-expressing mPFC neurons were optically excitable (Supplementary Fig. 15) and optically evoked mPFC-to-NAc EPSCs were readily detectable (Supplementary Fig. 16), demonstrating that optical activation of the mPFC-to-NAc inputs induced glutamate release, but did not support optical self-stimulation.

To determine whether quantitative differences existed in the amount of glutamate released from these two pathways, fluorescence-guided, whole-cell recordings in the NAc were performed while varying the light-stimulus intensity, in separate groups of mice selectively expressing ChR2 in either the BLA or the mPFC-to-NAc pathway. In NAc neurons that showed clear light-evoked EPSCs, BLA-to-NAc-evoked EPSCs had approximately twice the amplitude of those evoked after mPFC-to-NAc stimulation at maximal light intensities (Fig. 4d). In addition, NAc neurons typically showed excitatory postsynaptic responses to both optical stimulation of BLA inputs and electrical stimulation of cortical afferents (Supplementary Fig. 17), indicating that medium spiny neurons in the NAc receive both mPFC and BLA inputs, but that mPFC inputs release less glutamate.

These results show that selective activation of BLA, but not mPFC, glutamatergic inputs to the NAc promotes motivated behavioural responding. This is consistent with the hypothesized role of BLA inputs in facilitating responding to cues, and of mPFC inputs in suppressing inappropriate actions[16]. Dopamine signalling that is capable of activating D1Rs during optical self-stimulation sessions could arise from the burst-firing of dopaminergic neurons, time-locked to salient stimuli during behavioural responding[17,18]. Alternatively, glutamate released from BLA terminals may gate the release of dopamine from dopaminergic fibres in the NAc directly, independently of neuronal activity in the ventral tegmental area[19,20]. Our results show that afferent-specific glutamatergic neurotransmission from the BLA to the NAc is both necessary and sufficient to promote the expression of motivated behavioural responding.

METHODS SUMMARY

Opsin delivery to neural tissue. The adeno-associated viruses AAV-Camk2α–ChR2–EYFP, AAV-Camk2α–EYFP and AAV-Camk2α–NpHR3.0–EYFP were packaged as AAV5 by the University of North Carolina vector core facility. Virus (0.5 μl) was stereotactically injected into the BLA or mPFC at a rate 0.1 μl min^{-1} via 26-gauge injector needles coupled to a 2 μl Hamilton syringe. Mice were used for experiments about 28 d after virus injections.

Brain-slice electrophysiology. Opsin-expressing mice were deeply anaesthetized, decapitated and 200 μm sections of the BLA, NAc or mPFC were prepared. Whole-cell voltage-clamp recordings were performed using a caesium methylsulphonate internal solution and current-clamp recordings were performed using a potassium gluconate internal solution. One to five ms of 473-nm, 532-nm or 593.5-nm light was delivered via a fibre-coupled laser.

***In vivo* optogenetic stimulation and inhibition during behaviour.** Mice injected with opsin-encoding viral constructs were implanted with guide cannulae or chronic optical fibres directly above the NAc. Acute or chronic optical implants were connected to optical patch cables coupled to 473-nm or 532-nm lasers that were modulated by a stimulus pulse generator. The onset of laser pulses was controlled by signal pulses generated by behavioural hardware (Med Associates).

Full Methods and any associated references are available in the online version of the paper at www.nature.com/nature.

Received 30 January; accepted 10 May 2011.
Published online 29 June 2011.

1. Balleine, B. W. & Killcross, S. Parallel incentive processing: an integrated view of amygdala function. *Trends Neurosci.* **29,** 272–279 (2006).
2. Maren, S. & Quirk, G. J. Neuronal signalling of fear memory. *Nature Rev. Neurosci.* **5,** 844–852 (2004).
3. LeDoux, J. The emotional brain, fear, and the amygdala. *Cell. Mol. Neurobiol.* **23,** 727–738 (2003).
4. Cador, M., Robbins, T. W. & Everitt, B. J. Involvement of the amygdala in stimulus-reward associations: Interaction with the ventral striatum. *Neuroscience* **30,** 77–86 (1989).
5. Tye, K. M., Stuber, G. D., de Ridder, B., Bonci, A. & Janak, P. H. Rapid strengthening of thalamo-amygdala synapses mediates cue-reward learning. *Nature* **453,** 1253–1257 (2008).
6. Ambroggi, F., Ishikawa, A., Fields, H. L. & Nicola, S. M. Basolateral amygdala neurons facilitate reward-seeking behavior by exciting nucleus accumbens neurons. *Neuron* **59,** 648–661 (2008).
7. Di Ciano, P. & Everitt, B. J. Direct interactions between the basolateral amygdala and nucleus accumbens core underlie cocaine-seeking behavior by rats. *J. Neurosci.* **24,** 7167–7173 (2004).
8. Zhang, F., Wang, L. P., Boyden, E. S. & Deisseroth, K. Channelrhodopsin-2 and optical control of excitable cells. *Nature Methods* **3,** 785–792 (2006).
9. Phillips, P. E., Stuber, G. D., Heien, M. L., Wightman, R. M. & Carelli, R. M. Subsecond dopamine release promotes cocaine seeking. *Nature* **422,** 614–618 (2003).
10. Stuber, G. D. *et al.* Reward-predictive cues enhance excitatory synaptic strength onto midbrain dopamine neurons. *Science* **321,** 1690–1692 (2008).
11. Tsai, H. C. *et al.* Phasic firing in dopaminergic neurons is sufficient for behavioral conditioning. *Science* **324,** 1080–1084 (2009).
12. Di Ciano, P., Cardinal, R. N., Cowell, R. A., Little, S. J. & Everitt, B. J. Differential involvement of NMDA, AMPA/kainate, and dopamine receptors in the nucleus accumbens core in the acquisition and performance of pavlovian approach behavior. *J. Neurosci.* **21,** 9471–9477 (2001).
13. Gradinaru, V. *et al.* Molecular and cellular approaches for diversifying and extending optogenetics. *Cell* **141,** 154–165 (2010).
14. Wright, C. I. & Groenewegen, H. J. Patterns of convergence and segregation in the medial nucleus accumbens of the rat: relationships of prefrontal cortical, midline thalamic, and basal amygdaloid afferents. *J. Comp. Neurol.* **361,** 383–403 (1995).
15. McFarland, K., Lapish, C. C. & Kalivas, P. W. Prefrontal glutamate release into the core of the nucleus accumbens mediates cocaine induced reinstatement of drug-seeking behavior. *J. Neurosci.* **23,** 3531–3537 (2003).
16. Kalivas, P. W., Volkow, N. & Seamans, J. Unmanageable motivation in addiction: A pathology in prefrontal-accumbens glutamate transmission. *Neuron* **45,** 647–650 (2005).
17. Schultz, W. Predictive reward signal of dopamine neurons. *J. Neurophysiol.* **80,** 1–27 (1998).
18. Bromberg-Martin, E. S. & Hikosaka, O. Midbrain dopamine neurons signal preference for advance information about upcoming rewards. *Neuron* **63,** 119–126 (2009).
19. Floresco, S. B., Yang, C. R., Phillips, A. G. & Blaha, C. D. Basolateral amygdala stimulation evokes glutamate receptor-dependent dopamine efflux in the nucleus accumbens of the anaesthetized rat. *Eur. J. Neurosci.* **10,** 1241–1251 (1998).
20. Jones, J. L. *et al.* Basolateral amygdala modulates terminal dopamine release in the nucleus accumbens and conditioned responding. *Biol. Psychiatry* **67,** 737–744 (2010).
21. Paton, J. J., Belova, M. A., Morrison, S. E. & Salzman, C. D. The primate amygdala represents the positive and negative value of visual stimuli during learning. *Nature* **439,** 865–870 (2006).
22. Shabel, S. J. & Janak, P. H. Substantial similarity in amygdala neuronal activity during conditioned appetitive and aversive emotional arousal. *Proc. Natl Acad. Sci. USA* **106,** 15031–15036 (2009).
23. Tye, K. M. *et al.* Amygdala circuitry mediating reversible and bidirectional control of anxiety. *Nature* **471,** 358–362 (2011).
24. Shiflett, M. W. & Balleine, B. W. At the limbic-motor interface: disconnection of basolateral amygdala from nucleus accumbens core and shell reveals dissociable components of incentive motivation. *Eur. J. Neurosci.* **32,** 1735–1743 (2010).
25. Setlow, B., Holland, P. C. & Gallagher, M. Disconnection of the basolateral amygdala complex and nucleus accumbens impairs appetitive pavlovian second-order conditioned responses. *Behav. Neurosci.* **116,** 267–275 (2002).

Supplementary Information is linked to the online version of the paper at www.nature.com/nature.

Acknowledgements We thank J. Phillips, V. Kharazia, A. Adamantidis and H.-C. Tsai for assistance and advice. We also thank V. Gukassyan and the UNC Neuroscience Center microscopy core facility. This study was supported by funds from NARSAD, ABMRF, The Foundation of Hope, and NIDA (DA029325), by startup funds provided by the Psychiatry Department at UNC Chapel Hill (G.D.S.) and by the State of California through the University of California at San Francisco (A.B.). D.R.S. was supported by F32AA018610.

Author Contributions G.D.S. and A.B. designed, discussed and planned all experiments. G.D.S., D.R.S., A.M.S., W.A.v.L., J.E.H., S.C., K.M.T. and K.A.K. performed experiments. G.D.S., D.R.S., A.M.S. and W.A.v.L. analysed data. F.Z. and K.D. provided resources and training to G.D.S. G.D.S. and A.B. wrote the manuscript.

Author Information Reprints and permissions information is available at www.nature.com/reprints. The authors declare no competing financial interests. Readers are welcome to comment on the online version of this article at www.nature.com/nature. Correspondence and requests for materials should be addressed to G.D.S. (gstuber@med.unc.edu).

METHODS

Experimental subjects and stereotaxic surgery. Adult (25–30 g) male C57BL/6J mice (Jackson Laboratory) were group-housed until surgery. Mice were maintained on a 12 h:12 h light:dark cycle (lights on at 7:00). After the animals were acclimatized to the animal facility for ~1 week, they were anaesthetized with 150 mg kg^{-1} ketamine and 50 mg kg^{-1} xylazine and placed in a stereotaxic frame (Kopf Instruments). Microinjection needles were then inserted bilaterally directly above the BLA (coordinates from Bregma: −1.6 AP, ±3.1 ML, −4.9 DV). Microinjections were performed using custom-made injection needles (26-gauge) connected to a 2-μl Hamilton syringe. Each BLA was injected with 0.3–0.5 μl of purified and concentrated AAV (~10^{12} infectious units ml^{-1}) encoding ChR2–EYFP, NpHR3.0–EYFP or EYFP alone under the control of the *Camk2α* promoter. Injections occurred over 10 min followed by an additional 10 min to allow diffusion of viral particles away from the injection site. For optical self-stimulation experiments, mice were first injected unilaterally into the BLA with virus and then a guide cannula was implanted directly over the ipsilateral NAc (+1.3 AP, ±1.0 ML, −4.0 DV) to allow insertion of the fibre-optic cable during the experiment. The fibre was secured to the skull using Geristore (http://www.denmat.com) dental cement. Mice were then returned to their home cage. Body weight and signs of illness were monitored until recovery from surgery (approximately 2 weeks). All procedures were conducted in accordance with the guide for the care and use of laboratory animals, as adopted by the NIH, and with approval of the UNC and UCSF institutional animal care and use committees.

Construct and AAV preparation. DNA plasmids encoding pAAV-Camk2α–ChR2–EYFP (H134R), pAAV-Camk2α–NpHR3.0–EYFP or pAAV-Camk2α–EYFP were obtained from the laboratory of K. Deisseroth (see http://www.optogenetics.org for additional details). Plasmid DNA was amplified, purified and collected using a standard plasmid maxiprep kit (Qiagen). After plasmid purification, restriction digest and sequencing to confirm DNA fidelity, purified recombinant AAV vectors were serotyped with AAV5 coat proteins and packaged by the UNC vector core facilities using calcium phosphate precipitation methods. The final viral concentration was 1–2 × 10^{12} viral particles ml^{-1}.

Slice preparation for patch-clamp electrophysiology. Mice were anaesthetized with pentobarbital and perfused transcardially with modified artificial cerebrospinal fluid containing 225 mM sucrose, 119 mM NaCl, 2.5 mM KCl, 1.0 mM NaH_2PO_4, 4.9 mM $MgCl_2$, 0.1 mM $CaCl_2$, 26.2 mM $NaHCO_3$ and 1.25 mM glucose. The brain was removed rapidly from the skull and placed in the same solution used for perfusion, at ~0 °C. Coronal sections of the NAc or BLA (200 μm) were then cut on a vibratome (VT-1200, Leica Microsystems). Slices were placed in a holding chamber and allowed to recover for at least 30 min before being placed in the recording chamber and superfused with bicarbonate-buffered solution saturated with 95% O_2 and 5% CO_2 and containing 119 mM NaCl, 2.5 mM KCl, 1.0 mM NaH_2PO_4, 1.3 mM $MgCl_2$, 2.5 mM $CaCl_2$, 26.2 mM $NaHCO_3$ and 11 mM glucose (at ~32 °C).

Patch-clamp electrophysiology. Cells were visualized using infrared differential interference contrast and fluorescence microscopy. Whole-cell voltage-clamp or current-clamp recordings of BLA and NAc neurons were made using an Axopatch 200A or B amplifier. Patch electrodes (3.0–5.0 MΩ) were backfilled with internal solution containing 130 mM KOH, 105 mM methanesulphonic acid, 17 mM hydrochloric acid, 20 mM HEPES, 0.2 mM EGTA, 2.8 mM NaCl, 2.5 mg ml^{-1} MgATP and 0.25 mg ml^{-1} GTP (pH 7.35, 270–285 mOsM). Series resistance (15–25 MΩ) and/or input resistance were monitored online with a 4 mV hyperpolarizing step (50 ms) given between stimulation sweeps. All data were filtered at 2 kHz, digitized and collected using pClamp10 software (Molecular Devices). For current-clamp experiments to characterize cell firing, ten pulses at frequencies of 1, 5, 10 and 20 Hz, respectively, were tested to determine spike fidelity (the percentage of light pulses that lead to action potentials). For optical stimulation of EPSCs, stimulation (pulses of 1–2 mW, 473-nm light delivery via a 200-μm optical fibre coupled to a solid-state laser) was used to evoke presynaptic glutamate release from BLA projections to the NAc. NAc medium spiny neurons were voltage-clamped at −70 mV. For pharmacological characterization of glutamate currents, light-evoked EPSCs were recorded for 10 min, followed by bath application of 10 μM CNQX for an additional 10 min. Ten to twelve sweeps before and after drug addition were averaged and peak EPSC amplitudes were then measured. For EPSC pulse-train experiments, input-specific currents were evoked by 60 optical pulses (20 Hz stimulation, 5 ms pulse duration). This was repeated 12 times at 0.1 Hz. SCH23390 (4 μM) or vehicle was then bath-applied for 10 min and the stimulus train was repeated. The average EPSC train from the six sweeps immediately before drug application was then compared with the train for the six sweeps immediately after drug application.

***In vivo* optrode recording.** Approximately 21–28 d after bilateral injection of AAV-Camk2α–ChR2–EYFP into the BLA, mice were deeply anaesthetized with ketamine and xylazine and placed in a stereotaxic frame equipped with a temperature controller to regulate body temperature. The skull was then removed directly above the NAc. Parylene-coated tungsten electrodes (1 MΩ), attached with epoxy resin to an optical fibre of 200 μm core diameter and 0.37 numerical aperture coupled to a 473-nm laser, were then lowered into the NAc to record unit activity of postsynaptic medium spiny neurons after trains of light pulses were used to evoke BLA-to-NAc-specific glutamate release. Ten pulses of light (10–20 mW, 5 ms) at frequencies of 1, 5, 10 and 20 Hz, respectively, were used to determine spike fidelity *in vivo*, analogous to the experiment performed during whole-cell recording. Unit activity was amplified with an extracellular amplifier (A-M systems), band-pass filtered at 300 Hz low/5 kHz and digitized using pClamp10 software.

Freely moving optical self-stimulation. At 21–28 d after injection of pAAV-Camk2α–ChR2–EYFP or control virus into the BLA, mice with cannulae placed above the NAc were prepared for nose-poke training. Mice were mildly food-restricted to 4 g of food per day to stabilize body weight and facilitate behavioural responding. Body weight was monitored throughout the experiment and did not fall below ~90% of their free-feeding weight. Immediately before placing mice in the operant chambers, stylets were removed from the cannulae and a flat-cut 125-μm-diameter fibre-optic cable, coupled to a solid-state 473-nm laser outside the operant chamber, was inserted through the guide cannula and placed directly above the NAc. Immediately before insertion through the guide cannula, light output through the optical fibres was adjusted to 10–20 mW. The optical fibre was then secured into place via a custom-made locking mechanism to ensure that no movement of the fibre occurred during the experiment. Mice were then placed in standard Med-Associates operant chambers equipped with an active and inactive nose-poke operandum directly below two cue lights. The chambers were also equipped with house lights, audio stimulus generators and video cameras coupled to DVD recorders. A 1-h optical self-stimulation session began with the onset of the cue light above the active nose-poke operandum. Each active nose poke performed by the animal resulted in an optical stimulation of BLA-to-NAc fibres (60 pulses, 20 Hz, 5 ms pulse duration). Both active and inactive nose-poke time-stamp data were recorded using Med-PC software and analysed using Neuroexplorer and Microsoft Excel software.

NAc microinjections before optical self-stimulation. Stylets were removed from guide cannulae and a 26-gauge injector needle connected to a 1-μl Hamilton syringe was inserted. All microinjections were delivered in 0.3 μl sterile saline at a rate of 0.1 μl min^{-1}. Injector needles remained in place for an additional 2 min before being removed and replaced immediately with stylets or optical fibres for self-stimulation sessions. Doses of drugs used for microinjections were: 600 ng in 0.3 μl for SCH23390; 100 ng in 0.3 μl and 3 μg in 0.3 μl for raclopride; and 10 μg in 0.3 μl for lidocaine.

Implantable optical fibres for NpHR inhibition during behaviour. For these experiments, mice were bilaterally injected into the BLA with virus encoding NpHR3.0–EYFP or EYFP, as described above. Mice were also implanted with bilateral optical fibres targeted directly above each NAc. Optical fibres were constructed in-house by interfacing a 7–10-mm piece of 200-μm, 0.37-numerical-aperture optical fibre with a 1.25-mm zirconia ferrule (fibre extending 5 mm beyond the end of the ferrule). Fibres were attached with epoxy resin into the ferrules, then cut and polished. After construction, all fibres were calibrated to determine a percentage of light transmission at the fibre tip that would interface with the brain. Before bilateral implantation, fibres were matched to each other so that each fibre would output an equal amount of light (to within 10%). This was done to ensure that an equal amount of light was delivered to each hemisphere. After surgery, protective plastic caps were placed on the implanted optical fibres to protect them from dust and debris.

Four to five weeks after implantation surgery and 3 d before the experiment, mice were connected to 'dummy' optical-patch cables each day for 30–60 min to habituate them to the tethering procedure in their home cage. On experiment days, protective caps were removed from the implanted fibres. Fibres were then connected to custom-made optical-patch cables (62.5 μm core diameter) that were covered with furcation tubing to protect the cables and prevent light from the laser from illuminating the operant chamber. Bilateral fibres were connected to a fibre splitter (50:50 split ratio) that interfaced with a fibre-coupled 532-nm DPSS laser (200 mW). On the basis of the calibration factor of each pair of fibres, light intensity was set to 10 mW illumination at each fibre tip in the brain.

Optical inhibition of BLA-to-NAc fibres during sucrose responding. Mice with optical fibres implanted above the NAc, and expressing either NpHR3.0–EYFP or EYFP in BLA-to-NAc fibres, were trained to drink sucrose in response to an environmental stimulus that predicted sucrose delivery. The start of the session was signalled by the onset of white noise in the operant chamber. Each session consisted of 50 cue–reward pairings with a random inter-trial interval of 120 s. During each trial, a digital pulse was sent from the behavioural hardware to engage the laser 200 ms before the onset of a 5-s reward-predictive stimulus (tone/house-light compound stimulus). Delivery of 20 μl of 20% sucrose to a receptacle

occurred immediately after the termination of the reward-predictive cue, and the laser pulse was terminated 200 ms after the cue ended. The laser pulse was started and extended for 200 ms before and after the cue on the basis of *in vitro* experiments in which we observed that activation of NpHR led to maximal inhibition 200 ms after the start of the laser pulse. Cue presentation, reward delivery, lick and laser time-stamps were stored as separate data arrays and analysed offline with Microsoft Excel and Neuroexplorer.

Time-locked licking behaviour was quantified for all mice. Mice that did not make at least 200 licks on at least one of the four conditioning sessions were excluded from analysis. This resulted in the removal of two NpHR and two EYFP mice from analysis. Time-locked lick histograms with 0.5-s time bins were then constructed from −10 s to 30 s, time-locked to the cue onset ($t = 0$). Lick rates were normalized to baseline periods using a *Z*-score procedure ($z = (x-\mu)/\sigma$) with μ being the average lick rate and σ, the standard deviation in the 10 s preceding the cue onset.

Data analysis. Statistical significance was assessed using *t*-tests or analysis of variance (ANOVA), followed by post-hoc tests when applicable, using $\alpha = 0.05$. Data were analysed using Microsoft Excel with the Statplus plugin and Prism (GraphPad Software).

Virus expression and histology. After behavioural experiments, mice were deeply anaesthetized with pentobarbital and perfused transcardially with PBS followed by 4% paraformaldehyde dissolved in PBS. Brains were removed carefully and fixed in 4% paraformaldehyde for an additional 24–48 h. Brains were transferred to 30% sucrose for 48–72 h before slicing 50 μm sections of the BLA or NAc on a freezing-stage microtome or cryostat. Slices were then washed three times in PBS for 5 min. Slices were then stained for 1 h with 2% Neurotrace fluorescent Nissl stain (Invitrogen; excitation 530 nm, emission 615 nm) diluted in PBS with 0.1% Triton X-100. Slices were then washed and mounted on gelatin-coated slides, treated with fluorescent-mounting media and mounted. Expression of ChR2–EYFP, NpHR3.0–EYFP or EYFP was then examined for all mice using either a Nikon inverted fluorescent microscope with a ×4, ×10 or ×20 objective or a Zeiss laser-scanning confocal microscope at ×25 and ×63. After injection of virus into the BLA, robust expression of ChR2–EYFP was observed in BLA projection targets including the NAc, mPFC, hippocampus, insular cortex and to a lesser extent, the dorsal medial striatum. Mice showing no EYFP expression in the NAc owing to faulty microinjections, and mice showing cannula or fibre placements outside the NAc, were excluded from analysis.

Reconstruction of optical stimulation or inhibition sites in the NAc. To determine optical stimulation sites in experiments in which guide cannulae were used to introduce optical fibres into brain tissue (BLA-to-NAc and mPFC-to-NAc optical self-stimulation experiments, see Supplementary Figs 3 and 14 for the location of optical stimulation sites), fixed and stained coronal brain sections (see above) containing the NAc and cannula tracks were examined on an upright conventional fluorescent microscope. Cannula tracks were located in the slices and optical stimulation sites were determined by locating the site 1 mm ventral to the end of the cannula tip. A 1-mm distance was used in these experiments because the optical fibres extended 0.5 mm beyond the end of the cannula (each fibre was cut to this length before insertion). On the basis of the light output from these optical fibres (477 mW mm^{-1} at the tip), and calculating intensity by taking into account geometric loss and scattering through tissue[1], loss at 0.5 mm beyond the fibre tip led to an estimated 2.6% transmission, or 12.4 mW mm^{-1} at this distance. At 1 mm from the tip of the optical fibre, estimated transmission dropped to 0.56% or 2.67 mW mm^{-1}, which approximates the minimum intensity required to activate opsin proteins (1 mW mm^{-1}). For NpHR-mediated inhibition experiments, optical inhibition sites (Supplementary Fig. 11) were determined in a similar fashion, with 0.5 mm used as the distance from the fibre tip to the diagrammed inhibition sites because no guide cannula was present. This distance represents the centre location where optical stimulation or inhibition occurs (0.5 mm above and below). All calculations were performed using equations and constants listed in ref. 21.

26. Aravanis, A. M. *et al.* An optical neural interface: *in vivo* control of rodent motor cortex with integrated fiberoptic and optogenetic technology. *J. Neural Eng.* **4,** S143–S156 (2007).